Engineering Solid Mechanics 11 (2023) 271-280

Contents lists available at GrowingScience

Engineering Solid Mechanics

homepage: www.GrowingScience.com/esm

The effect of hardness matching of rail/wheel materials on wear rate of railway wheel

Hewan Getachew Yenealem[a*], Daniel T. Redda[b] and Awel Mohammedseid[c]

[a]*African Railways Center of Excellency, Addis Ababa Institute of Technology, Addis Ababa University, Ethiopia*
[b]*Associate Professor in Mechanical Design, School of Industrial and Mechanical Engineering, Addis Ababa Institute of Technology, Addis Ababa University, Ethiopia*
[c]*African Railways Center of Excellency, Addis Ababa Institute of Technology, Addis Ababa University, Ethiopia*

ARTICLEINFO

Article history:
Received 1 October 2022
Accepted 16 March 2023
Available online
16 March 2023

Keywords:
Hardness matching
Rail/wheel materials
Wear performance
Hardness
Multi body simulation software

ABSTRACT

There is no rationalization for a certainty that harder wheels or rails will result in an increase in wear of the opposite side of the wheel/rail interface. This research investigated how the wear of wheel material changes when the hardness of the opposing pair is varied. Three Rail/wheel material matches; normalized UIC50 kg/m and S1002 wheel profile (Rail/wheel material 1), normalized UIC60 kg/m and whole heat treated S1002 wheel profile (Rail/wheel material 2) and rim heat treated UIC60 kg/m and whole heat treated S1002 wheel profile (Rail/wheel material 3) has been investigated using multi-body simulation software (SIMPACK) and MATLAB programming. For validation, as an experimental advantage, the wear depths measured on the wheel tread wear of the end vehicle of LRT for mileage of 50,000 km are compared to the results of numerical simulation performed. As a result, the estimated total tread wear amount after a mileage of 50,000 km is 4% larger than the experimental one. That is indeed a very good result considering that either component of the wheel wear prediction model used is neither adjustment nor calibration. From the three rail/wheel matches, Rail/wheel material 3 found to be the better material match that could resist wear significantly considering material hardness as important criteria for comparison. The study could remark that, despite the fact both wheel and rail material hardness could affect the wear performance in respected positive ways, most significant improvements are attained by improving the rail material hardness ahead of wheel material.

1. Introduction

In metallurgy hardness is defined as the ability of a material to resist plastic deformation. Hardness measurement can be defined as macro, micro or nano scale according to the forces applied and displacements obtained. There are three types of tests used with accuracy by the metals industry; they are the Brinell hardness test, the Rockwell hardness test, and the Vickers hardness test. Since the definitions of metallurgic ultimate strength and hardness are rather similar, it can generally be assumed that a strong metal is also a hard metal. A number of different techniques have been used for studying wear of railway wheel steels. The wheels of railway vehicles are subjected to wear for the duration of train operation. When the worn state of the profiles reaches a limit value, the wheels have to be re-profiled. Apparently, the railway wheels can only be re-profiled 3 or 4 times. The excessive wheel wear implies that, conversely, also the rails are subjected to premature deterioration. There have been a number of studies, both small and full-scale, to investigate how wear changes as the different standard grades of wheel and rail material are run against each other. Wear assessment of wheel materials as well as wear rates, regimes and transitions was carried out by R. Lewis et al. (Lewis et al., 2005). They use twin disc wear testing extensively for studying wear of wheel and rail materials. Wear rates are seen to increase steadily initially, before increasingly rapidly as the severity of the contact

* Corresponding author. Tel.: +251920253055, +251960541313
E-mail addresses: hewan.getachew@aait.edu.et (H. G. Yenealem)

ISSN 2291-8752 (Online) - ISSN 2291-8744 (Print)

doi: 10.5267/j.esm.2023.3.002

conditions is increased. Temperature calculations for the contact showed that the large increase in wear rates seen at the second wear transition may result from a thermally induced reduction in yield strength and other material properties. Wear maps have been produced that improved understanding of wheel wear mechanisms and transitions and will help in the aim of eventually attaining a wear modelling methodology reliant on material properties rather than wear constants derived from testing. A new high wear resistance and RCF resistance rail (SP3) was developed by KIMURA Tatsumi et al. (Kimura et al., 2011) for heavy haul freight railways in North America and other countries. The pearlite lamellar spacing of the developed SP3 rail is extremely fine, at 0.07 μm, and hardness is also high, being HB420 points or higher in the Brinel scale at the rail head surface and HB370 or higher at a depth of 1 inch (25.4 mm). As a result, an improvement or 10% or more in wear resistance was confirmed in comparison with the conventional heat treated rail in both laboratory tests and a performance confirmation test. A review of how wear of wheel and rail material is affected by changing hardness of the opposite material has been carried out by Wenjian Wang et al. (Lewis et al., 2016). As a result, where the rail is softer than the wheel; rail wear decreases with increasing rail hardness, and wheel wear increases. Where the rail is harder than the wheel, again rail wear decreases with increasing rail hardness, but wheel wear remains constant. In both cases, however, as rail hardness increases overall system wear reduces. Windarta *et al.* (2011) used a pin on the disc to determine the influence of load on wear rate and wear mechanism in rail steel materials (Liu et al., 2016). The study used the same material for pin and disk testing under a rotating speed of 100rpm. The experimental results show that the wear rate increases with the proportionality coefficient of 0.1135 with the increasing of applied loads.

Consistent with the work conducted by different Laboratories, different rail types have different influences on the wear of wheels. This finding supports greatly that a proper test should be performed while selecting the right wheel/rail material combination. In this research the effects of hardness matching of rail/wheel materials on the wear performances of railway wheels are studied. The focus is on the development of better wheel-rail material matching that could resist wear significantly. Three kinds of rail and wheel steels with respect to their rail/wheel matches were tested to investigate the wear behaviours of wheel materials running on Ethiopia-Addis Ababa Light Rail Transits (LRT) line. Normalized UIC50 kg/m and S1002 wheel profile (Rail/wheel material 1), normalized UIC60 kg/m and whole heat treated S1002 wheel profile (Rail/wheel material 2) and rim heat treated UIC60 kg/m and whole heat treated S1002 wheel profile (Rail/wheel material 3) have been studied using multi-body simulation software (SIMPACK) and MATLAB programming. The methodology results are validated against the vehicle's specifications; derailment of coefficient and maximum lateral force. As an experimental advantage, the wear depths measured on the wheel tread wear of the end vehicle of LRT for mileage of 50,000 km are compared to the results of numerical simulation performed.

2. Methodology

Wear prediction models expose the wheel to contact situations; it is likely to be encountered in reality when travelling a rail network or a certain route, by means of simulations. The methodology is based on wheel wear simulations, which are chosen to reflect the actual rail network for the vehicle, including vehicle and track design geometry and irregularity, both wheel and rail profiles and the vehicle operating conditions (Jin & Ahmadian, 2013). Firstly, Creep force and crepages are determined from vehicle motion analysis using SIMPAC. Next, the output from the vehicle–track simulations, which are normal forces, size of contact ellipse semi-axis, contact patch location (lateral coordinate of center) and crepages (including spin), form the input to a wear model. The wear model then relates the quantities in the contact surface to a wear depth on the profile and then a wear distribution is calculated. Wear depth is calculated to create a worn wheel profile. Lastly, both the wear distribution as well as the new wheel profile is smoothed in every wear step by using a cubic spline interpolation algorithm. Then, the updated (worn) profile serves as the initial profile in the following wear step and step is then repeated until the desired running distance is attained. To avoid the possibility of the predicted wheel profile deviating into unrealistic shapes, the maximum allowed wear depth perpendicular to the profile is set to 0.1 mm. Wear mechanism of rail/wheel materials compositions will be verified and new wheel-rail combinations will get determined. Fig. 1 shows the wheel wear prediction Methodology.

3. Application

The present wear prediction tool is applied to a vehicle operating the commuter rail network in Ethiopia (AALRTs). The first light rail line in Addis Ababa was opened for revenue service on September 20. The network is operated by a fleet of 41 three-section 70% low-floor trams. With trams running at up to 70 km/h, the two routes (one being the East-west and the other North-South lines) are designed to carry up to 15 000 passengers/h in each direction. The total length of the lines is 31.025km, where the East-West main line is around 16.99km long; the North-South main line is around 16.689km long. Both lines share a section of 2.662km. AALRT uses a double track dedicated for the service of passengers for both lines with a track gauge of 1435mm. The type of rails for main lines and depot is 50kg/m, the maximum super-elevation being 120mm and inclination at rail bottom 1/40. The axle load is ≤11 (1+3%) t. The trains operating in each route are identified by their vehicle number; trains operating in the East-West line start by vehicle number 2XX and trains operating in the North-South line start by vehicle number 1XX. Fig. 2 shows the Addis Ababa LRT train running on the rail line.

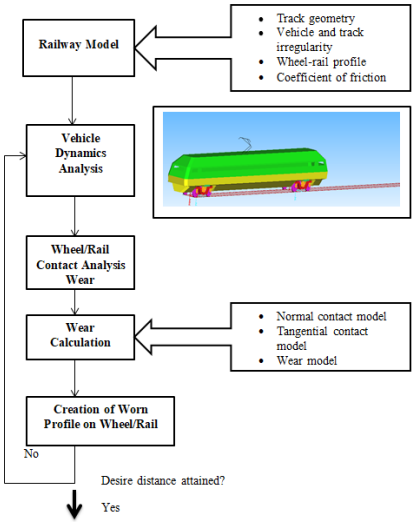

Fig. 1. Methodology of wheel wear prediction tool

Fig. 2. LRT train running on the rail line

The vehicles are 70% low-floor articulated 6-axle modern trams with two tramcars that are able to operate with double heading. The maximum operation speed of the vehicle is 70 km/hr with average travelling speed of 20 km/hr average dwelling time of 30 seconds at each station. The ride quality of the vehicle is < 2.5; coefficient of derailment of the vehicle is < 0.8. The longitudinal vehicle jerk rate is < 1.0 m/s^3.

Table 1. Chemical Composition of Candidate wheel and Materials

Predicted wheel and rail Materials			Chemical Composition %					Hardness (BHN)
			C	Si	Mn	P	S	
Rail/wheel material 1	wheel	Normalized UIC S1002	0.4	0.35	0.8	≤ 0.05	≤0.05	200
	rail	Normalized UIC50	0.6	0.3	0.8	≤0.05	≤0.05	240
Rail/wheel material 2	wheel	Normalized UIC S1002	0.6	0.35	0.8	≤ 0.05	≤ 0.05	200
	rail	Whole heat treated (very hard) UIC60	0.8	0.1	0.8	≤0.03	≤ 0.03	350
Rail/wheel material 3	wheel	Rim heat treated (hard)UIC S1002	0.6	0.1	1.3	≤ 0.04	≤ 0.04	260
	rail	Whole heat treated (very hard)UIC60	0.8	0.1	0.8	≤0.025	≤ 0.03	350

We set two new matching of rail/wheel materials from conventional wheel and rail materials and one matching of rail/wheel material with similar property with the Addis Ababa LRT specifications (Rail/wheel material 1). The wheel-rail material matches used for this wear analysis are selected based on their hardness properties and presented (table1).

4. Wear prediction model

The main objective is to investigate on hardness matching of rail/wheel materials of existing and new sets of wheel and rail material combinations by simulating them for wear performance analysis using both multi body simulation software (SIMPACK) and MATLAB programming. Three- dimensional multi-body models and a wear model have been used to predict wear for railway wheels running on a tangent line. Forces which the wheel and rail profiles could experience are provided from the dynamics simulations of the vehicle–track interaction. The wear model calculates the amount of wear on the wheel profiles using output from vehicle–track interaction simulations (forces, creepages, semi-axes of the contact ellipse) as an input. Then, the wear distribution and the new wheel profile are smoothed in every wear step using a cubic spline interpolation algorithm.

4.1 Vehicle–track interaction

Modelling of railway vehicles as multi-body systems (MBS) covers a wide range of problems, and the modelling describes the real system by a combination of rigid bodies, whereas their motions of the bodies are determined by joints and constraints, and force elements acting between the bodies (Kaiser, 2012). The multi-body simulations can be performed in a variety of commercial software, for example ADAMS/Rail, VAMPIRE, SIMPACK (Šlapák & Michálek, 2021). For the purpose of this paper, the multi-body simulations of railway vehicle models of the 80 km/h Addis Ababa Light Rail Transit, running was performed using the simulation software SIMPACK 2020.1. The model consists of a full dynamic rigid multi-body model

with a carbody, two bogie bolsters, two bogie frames, two traction link masses, four wheelsets, and eight axlebox connected by suspension elements, figure 3. The primary suspension consists of rocker type journal box positioning device with elastic joints connecting the axlebox to the bogie frame, and vertical damper with lower and upper stops. Air spring which is mounted in parallel on each side of the bogie frame is modeled as secondary suspension. The vehicle parameters and speed, the wheel and rail profiles, the track flexibility, the ideal geometry of the line and wheel and rail irregularities are the inputs of the multi-body program. Table 2 shows that the general technical parameters and condition of freight car of the national Railway of Ethiopia [Source: Railways corporation, rolling stocks specifications]

Table 2. Technical parameters of passenger car for Addis Ababa Light Railway Transit

Technical Values	Values
Railway Gauge	1435 mm
loading capacity	70 kg
Wheel Diameter	600 mm
Maximum speed	70 k/hr
Axle load	≤11（1+3%）tones
Minimum radius of vertical curve	1000 m
Maximum gradient	55%
Empty vehicle load	44 tone
Type of rails for main lines and depot	50 kg/m

(Source: Ethiopian Railway Corporation, technical specification of vehicle)

Track irregularities represent a kinematic excitation of the mechanical system of the vehicle during the run of a railway vehicle on a real track. Oscillation of the wheel forces around their static values during the run is a direct consequence of this effect. The static values of the wheel forces are given by the relevant axle load; amplitudes of the oscillations are influenced with the unsprung masses, vehicle speed and the track irregularities (Šlapák & Michálek, 2021).

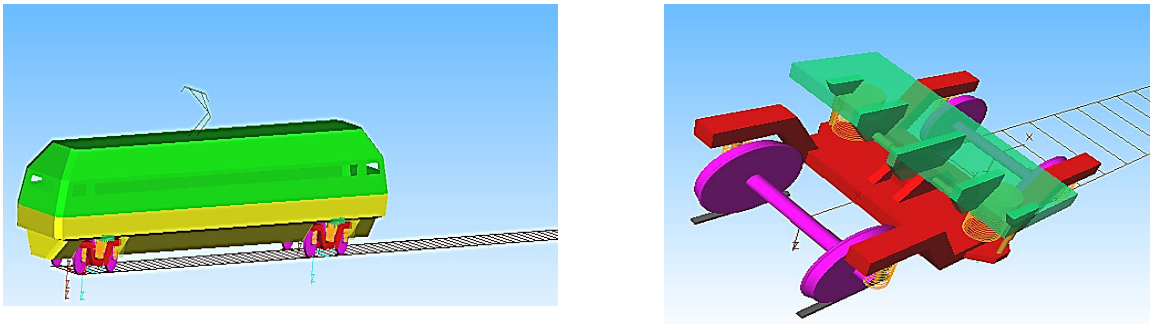

(a) (b)

Fig. 3. SIMPACK model, (a) bogie model (b) vehicle model

4.2 Wheel-rail contact modeling

The wheel/rail contact area is typically the size of a small coin and, commonly, eight such contacts (i.e., eight wheels) support a vehicle weighing from 30 t (lightweight passenger coach) to 140 t and more (heavy freight). The material in and around the contact area is therefore highly stressed. High rates of wear might be expected for such a contact but, in addition, because the load is applied and removed many times during the passage of each train (Vollebregt & Wilders, 2011). Different numerical approaches exist to estimate the normal force for a given contact patch. An ellipse is fitted in the contact area and the normal force is calculated for this ellipse using the Hertz theory which is known as the equivalent ellipse method. The computational effort using this method is very low which is very important in the field of railway simulation. The tangential problem is solved by the FASTSIM algorithm that is based on the simplified theory developed by Kalker and has been widely used in railroad vehicle computer programs (Vollebregt & Wilders, 2011). Creep is the ratio of sliding velocity (v) and vehicle speed (V). It can be broken down into three components: longitudinal Creep, lateral Creep, and Spin Creep (Dirks, 2015).

$$Longtudinal\ creep: \xi x = \frac{v_x}{V}, \tag{1}$$

$$Lateral\ creep: \xi x = \frac{v_y}{V}, \tag{2}$$

$$Spin\ creep: \varphi = \frac{\omega}{V}. \tag{3}$$

where ξx, ξy, and φ longitudinal, lateral and spin creepages, respectively. Creep forces are non-linear function of creepage and spin in the contact area with a maximum value of μN. however, the problem can be regarded as linear when the creepage is assumed to be small (Orvnäs, 2005).

4.3 Archard's wear law

The Archard wear equation is based on the theory of asperity contact, and was developed much later than energy dissipative hypothesis, though both came to the same physical conclusions, that the volume of the removed debris due to wear is proportional to the work done by friction forces. In present study, the amount of wear is calculated by adopting Archard's law (Jin & Ahmadian, 2013; Meghoe et al., 2008; Santamaria et al., 2009; Telliskivi & Olofsson, 2004) combined with FASTSIM, which is used to determine the distribution of slip velocities and sliding distances in the contact patch used as input in Archard's law. Archard's wear model suggests that the volume of material worn away is proportional to the sliding distance times the normal force and inversely proportional to the hardness of the worn material (Jiang et al., 2019).

$$V_{wear} = ki\frac{s\,.\,N}{H}, \tag{4}$$

where $k_i$is the wear coefficient [-], *s*[m] the sliding distance [m], *N* the normal force [N] and *H* the hardness of the material [N/m2]. k_i can be described as (Dirks, 2015),

$$k_i = \frac{(W/\rho)\,.\,H}{F}, \tag{5}$$

The wear coefficient k_i can be determined with the sliding velocity and contact pressure. According to Archard, Since the sliding distance is zero (zero sliding velocity), there is no wear on the sticking area of the contacts (Jin & Ahmadian, 2013)(Dirks, 2015). The wear depth for each cell element (Δz [m]) could be calculated:

$$\Delta z = k\,.\frac{\rho_z\,.\,\Delta s}{H} \tag{6}$$

where ρ_z is the contact pressure in [N/m^2]. The wear depth, Δz, is assumed that the initial wear acts in the direction normal to the undeformed wheel and rail profile. The sliding distance Δs can be treated as the distance that a wheel particle slides through the concerned cell element.

5. Result and discussion

5.1 Model validation

The modeled Ethiopian- Addis Ababa Light Rail Transits (LRT) vehicle is simulated on a straight track with a running speed of 70 km/hr. For validation of the wear prediction model of this study, before we proceed to the main scenario modeling and simulation, the results are validated against the vehicle's specifications, derailment of coefficient and maximum lateral force. The derailment coefficient measures the derailment safety by using the ratio between the lateral Y and the vertical (normal to the top of rail plane) Q components of the contact forces acting on the flanging wheel, the so-called derailment coefficient Y/Q (Diana et al., 2016; W. Zhang, 2020). The limit value for the derailment coefficient is often based on the famous formula due to Nadal (Diana et al., 2016).

$$\left(\frac{Y}{Q}\right)_l = \frac{tg\gamma_{MAX} - \mu}{1 + \mu tg\gamma_{MAX}} \tag{7}$$

with μ the wheel-rail friction coefficient and MAX γ the maximum contact angle which depends on the wheel and rail profiles. From Fig. 4(a), it can be observed that derailment of coefficient satisfies the standard (Y/Q < 0.8). Accordingly, in Fig. 4(b), the lateral force also fulfills the standard Y < 60 KN according to UIC 518, 2005.

5.2 Field Measurements

Rail transport safety mainly depends on the physical condition of vehicles and the rail infrastructure conditions. It is crucial to perform maintenance activities in accordance with instructions included in the individual technological processes which directly impacts the operational and rail transport safety, to a minimum (Kalinowski et al., 2021). The wheelset is an essential

part of the bogie and also one of the most severely worn parts of the vehicle which transfers the vehicle weight to the rails directly (H. Zhang et al., 2022). The dimensions of important structures of the wheel need to be measured during maintenance.

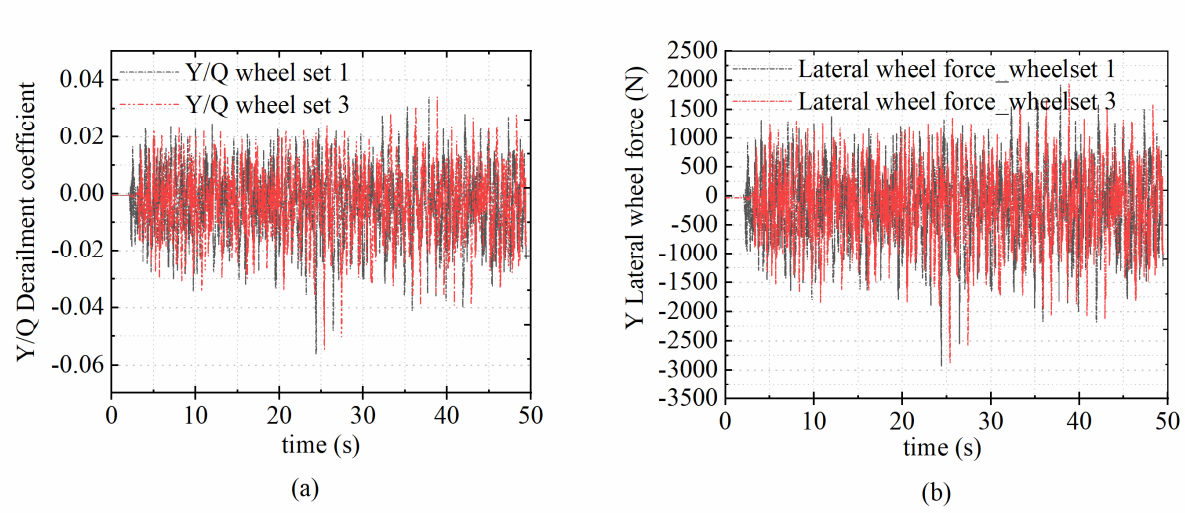

Fig. 4. (a) Derailment coefficient of wheelset 1 and 3, and (b) Lateral force of wheelset 1and 3.

The estimation of wear at the wheel–rail contact patch is mainly correlated with maintenance activities, train stability, and the possibility of carrying out specific strategies for wheel optimization (D. Zhang et al., 2014). In Ethiopia - Addis Ababa Light Rail Transits (LRT), daily, annual, quarterly, and monthly maintenance of vehicles are carried out at depots. Daily inspections of vehicles are lighting checking and the appearance of the entire bogie. The overhaul maintenance workshop contains a load tester and fixed/movable lifting jack, during which overhaul maintenance of vehicles and load testing take place. At the wheel re-profiling workshops, re-profiling activities are carried out using underfloor wheel lathe machines. The wear of wheels on the Addis Ababa Light Rail Transits (LRT) line were measured using a tread wear measuring device Electronic gauge (caliper), figure 5. Measurements are made directly on rolling stock without wheel set roll-out. The measurement of the diameter is performed according to the 'three points' technique, without the complete wheel coverage. The Electronic gauge contains a numeric display to show the wheel diameter value and also contains Bluetooth interface for transfer results into wheelset wear database management system.

Fig. 5. Railway wheel wear measurement at Addis Ababa Light Rail Transits (LRT); (a) Re-profiling workshop (b) electronic gauge (caliper) (c) Numeric display to show the wheel diameter value.

The wheel wear measurements were undertaken at the Kality wheel re-profiling workshop by LRT technicians from February 2016 to December 2016.Complete measurements of wheel tread diameter were taken before and after machining of the wheels. Five vehicles with average running mileage of 50,000 km were inspected at Ayat depot. Table 2 shows the summary of vehicles that were inspected at Kality depot with thread diameters.

5.3 Comparisons with field measurements

A number of different techniques have been used for studying wear of railway wheels and rail steels. Field measurements have been used in the past to study the causes of wheel and rail wear (Lewis et al., n.d.). This experimental study follows the profile evolution of wheels during some period in service and, the worn profiles and wear rate on the tread were the main concerns. FASTSIM is used to determine the distribution of slip velocities and sliding distances in the contact patch used as

input in Archard's law. The wear analysis is completed with the superposition between nominal and worn wheel profiles to evaluate the wear rate and mechanism of each rail/wheel matches on the railway wheel. The field data show that the wheel tread wears of the end vehicle are characteristic of their kind. So, these quantities, wheel profile wear parameters are compared here with the field data related to the end vehicle of the train. In Figure 6 the wear depths measured on the eight wheels of the end vehicle for a mileage of 50,000 km are compared to the results of numerical simulation performed. As we have seen from the computational, the results of the numerical simulations performed using the wheel profile wear prediction models are in very good agreement with the measurements. In fact, the estimated total tread wear amount after a mileage of 50,000 km is 4% larger than the experimental one. That is indeed a very good result considering that either component of the wheel wear prediction model used is neither adjustment nor calibration. Also the inaccuracy of the profilometer used to measure the wheel transversal profile should be taken into account.

Table 2. Addis Ababa Light Rail Transits (LRT) - Kality depot vehicles inspected between February 2016 and December 2016 Vehicle

Vehicle No.	Tread diameter (Td) in mm											
	WS 1	WS 2	WS 3	WS 4	WS 5	WS 6	WS 7	WS 8	WS 9	WS 10	WS 11	WS 12
212	659.7	659.6	659.7	659.4	660.1	660.1	660.1	660.2	659.3	659.9	659.6	659.5
205	659.4	659.5	659.6	659.3	660.2	660.2	660.0	660.0	659.6	659.6	659.6	659.7
215	659.6	660.0	659.8	659.7	660.3	660.4	660.1	660.3	659.8	659.8	659.8	659.6
208	659.4	659.5	659.6	659.8	660.1	660.3	660.2	660.1	659.7	659.6	659.4	659.6
218	659.3	659.6	659.3	659.4	660.2	660.2	660.1	659.9	659.1	659.7	658.9	659.3
210	659.0	659.3	659.4	659.2	660.1	660.3	650.7	650.9	659.3	659.5	659.2	659.2
Average Td/wheel	659.4	659.59	659.6	659.5	660.2	660.3	658.5	658.6	659.5	659.69	659.42	659.48

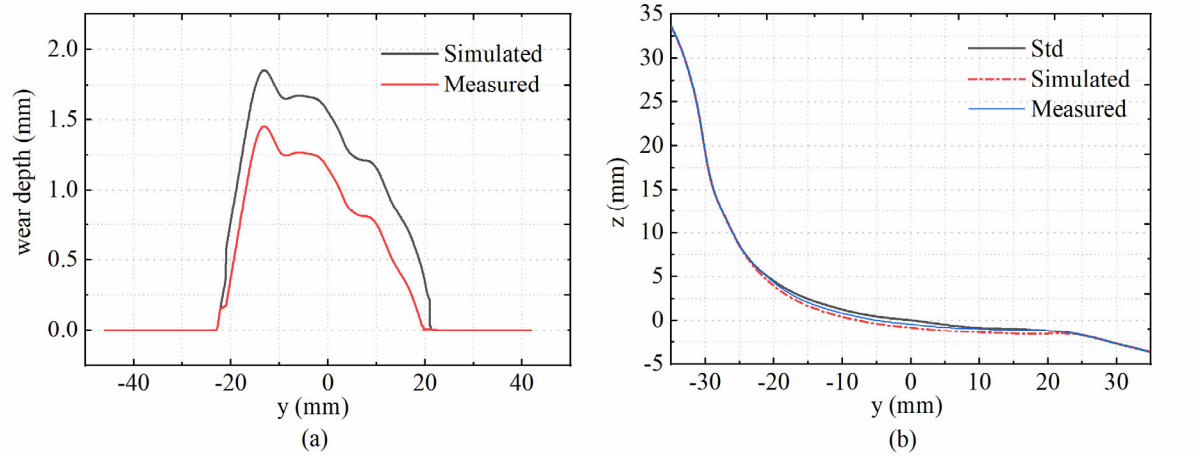

Fig. 6. a) Comparison superposition between simulated and measured wheel profile wear of rail/wheel maching of AALRTs at the end vehicle for amileage of 50,000 km b) Comparison between simulated and measured wheel profile wear depths rail/wheel maching of AALRTs at the end vehicle for a mileageof 50,000 km.

5.4 Analysis and Prediction of Simulation Results

Fig. 8 illustrates LRT wheel tread wear for different mileage and comparison of wheel tread wear measurements of three candidate rail/wheel matches. Fig. 8 (a) shows the current Addis Ababa LRT wheel profile for 50000 km, 10000 km, 15000 km and 20000km. These model results are compared with the experimental results and validated with a very good agreement (section 5.3.). On the other hand, Fig. 7 (b) shows that comparison of wheel tread wear measurements of three candidate rail/wheel matches at the end vehicle for mileage of 200,000 km of a low-speed train at run especially on Addis Ababa Light Rail Transits. This represents the life-length of an average wheelset. Considering the overall computational analysis the wear rate has been improved as of the increment of the wheel and rail material hardness. Fig. 8 illustrates the influence of hardness on the wear depth of three candidate rail/wheel machining materials on wheel material for different mileage. For the sake of clear understanding, we summarized the results (Fig. 7 & Fig. 8) grouping into three states of affairs. In this way, it is possible to overlook the effect of rail material hardness as of the fixed wheel material hardness, matching of normalized UIC50 kg/m and S1002 wheel profile (Rail/wheel material 1) verses whole heat treated UIC60 kg/m and normalized S1002 wheel profile (Rail/wheel material 2), (scenario 1). In this scenario, in both cases the wheel materials have the same hardness, whereas the

rail material hardness has to be changed from 240BHN to 350BHN. The estimated total tread wear amount after a mileage of 200,000 km is improved by 0.557 mm on rail/wheel material matching of Rail/wheel material 2 (normalized S1002/whole heat treated UIC60 kg/m). These numbers are the indication of the rail material hardness effect intensity on the wear performance improvement. In scenario 2 on the other hand could possible to examine the effect of wheel material hardness by taking constant rail material hardness matching of normalized S1002/ whole heat treated UIC60 verses rim heat treated S1002/ whole heat treated UIC 60 kg/m (Rail/wheel material 2 and Rail/wheel material 3). In the other words, in both combinations the rail material hardness is the same but the wheel material hardness has to be changed from 200BHN to 260BHN. The estimated total tread wear amount of Rail/wheel material 2 after a mileage of 200,000 km is improved by 0.5 mm on rail/wheel material matching of Rail/wheel material 3. This indicates that within the experimentally accepted range, the increment of the wheel material hardness could have significant effect on the wear performance improvement. In the last scenario (scenario 3), it could be possible to investigate both wheel and rail material hardness effects by comparing the wear rate performance against the existing AALRT's wheel-rail material combinations wear performance (Rail/wheel material 1 and Rail/wheel material 3). In rail/ wheel matching of Rail/wheel material 3 both wheel and rail hardness has to be changed or raised by 60BHN and 110BHN respectively as compared to Rail/wheel material 1. As per this accentuated raise the wear performance has got to improve by 1.1mm. This output values are an indication of the wheel and rail material hardness significant effect on the performance of wear rate, bearing in mind the proportion of wheel-rail material hardness do matter the most.

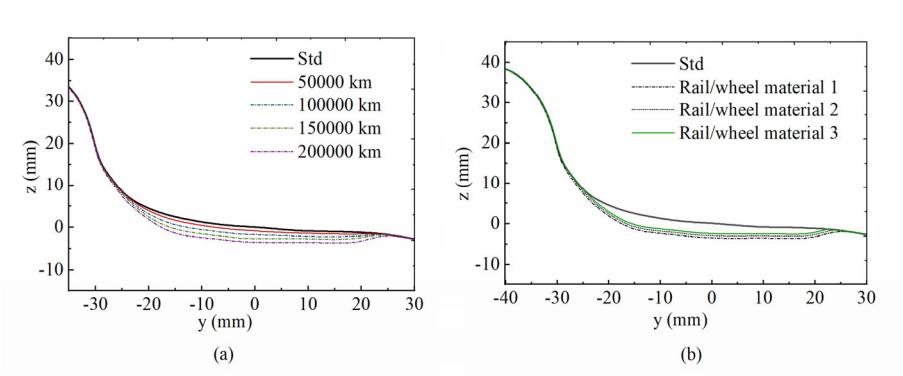

Fig. 7. Profile wear; (a) LRT wheel tread wear for different mileage (b) comparisons of wheel tread wear measurements of three candidate rail/wheel matches at the end vehicle for mileage of 200,000 km of a low-speed train at run especially on Addis Ababa Light Rail Transits.

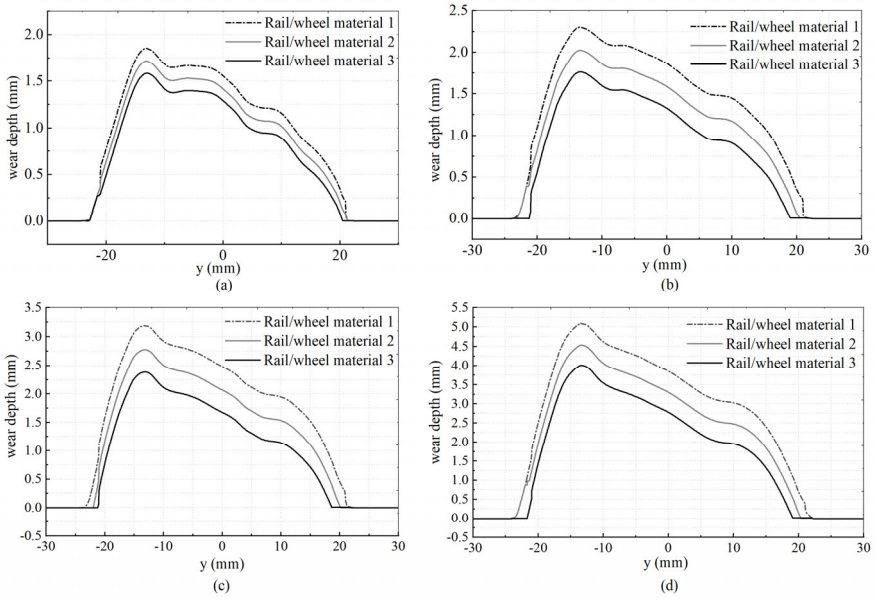

Fig. 8. comparisons of wheel wear depth of three candidate rail/wheel matches of a low-speed train at run especially on Addis Ababa Light Rail Transits. a) at the end vehicle for mileage of 50,000 km b) at the end vehicle for mileage of 100,000 km c) at the end vehicle for mileage of 150,000 km d) at the end vehicle for mileage of 200,000 km

6. Conclusion

Depending on the investigation that has been performed in three candidate rail/wheel matches, matching of normalized UIC50 kg/m rail and S1002 wheel profile (Rail/wheel material 1), hole heat treated UIC60 kg/m rail and normalized S1002 wheel profile (Rail/wheel material 2) and whole heat treated UIC 60 kg/m rail and rim heat treated S1002 wheel profile (Rail/wheel material 3), the following conclusions has been made.

- Whole heat treated UIC 60 kg/m rail and rim heat treated S1002 wheel profile matching (Rail/wheel material 3) found to be the better material match that could resist wear significantly considering material hardness as important criteria for comparison.

- Despite the fact both wheel and rail material hardness could affect the wear performance in respected positive ways, most significant improvements are attained by improving the rail material hardness ahead of wheel material (i.e. for enhanced wear performance, it is very important to made a material combination in a proportion that a relatively softer material (wheel) should roll on relatively harder material (rail).

- There is an indication that within the experimentally accepted range, the increment of the wheel material hardness could have a significant effect on the wear performance improvement.

- Since Rail/wheel material 3 has significant wear improvement relatively, this new wheel-rail material combination could be the most recommended that could improve the wear performance in Addis Ababa Light Rail Transits in substitution of the existing material combination, Rail/wheel material 1.

- Since this study is based on the computer aided experiment and the environmental factors were not considered in this simulation, those results accuracy couldn't be accountable as the actual operational results. So for the sake of accuracy those computational analyses should be supported by actual laboratory experiments as well.

Acknowledgement

The authors wish to extend their thanks to African Railways Center of Excellence (ARCE) for supporting this research.

Funding

World Bank Group

Availability of data and materials

The data underlying this article will be shared on reasonable request with the corresponding author.

Competing interests

The authors declare that they have no competing interests.

References

Diana, G., Bruni, S., Di Gialleonardo, E., Corradi, R., & Facchinetti, A. (2016). A study of the factors affecting flange-climb derailment in railway vehicles. *Civil-Comp Proceedings*, *110*(September 2019). https://doi.org/10.4203/ccp.110.63

Dirks, B. (2015). *Simulation and measurement of wheel on rail fatigue and wear*.

Jiang, Y., Zhong, W., Wu, P., Zeng, J., Zhang, Y., & Wang, S. (2019). Prediction of wheel wear of different types of articulated monorail based on co-simulation of MATLAB and UM software. *Advances in Mechanical Engineering*, *11*(6), 1–13. https://doi.org/10.1177/1687814019856841

Jin, X. C., & Ahmadian, M. (2013). Wheel wear predictions and analyses of high-speed trains. *Nonlinear Engineering*, *1*(3–4), 91–99. https://doi.org/10.1515/nleng-2012-0010

Kaiser, I. (2012). Refining the modelling of vehicle-track interaction. *Vehicle System Dynamics*, *50*(SUPPL. 1), 229–243. https://doi.org/10.1080/00423114.2012.671948

Kalinowski, A., Radek, N., & Bronček, J. (2021). SAFETY of OPERATION and MAINTENANCE ACTIVITIES of ROLLING STOCKS by the EXAMPLE of ELECTRIC MULTIPLE UNITS EN96. *Communications - Scientific Letters of the University of Žilina*, *23*(1), F11–F19. https://doi.org/10.26552/COM.C.2021.1.F11-F19

Kimura, T., Takemasa, M., & Honjo, M. (2011). Development of SP3 rail with high wear resistance and rolling contact fatigue resistance for heavy haul railways. *JFE Technical Report*, *16*(16), 32–37. https://doi.org/10.2320/materia.50.123

Lewis, R., Magel, E., Wang, W., Olofsson, U., Lewis, S., Slatter, T., & Beagles, A. (n.d.). *Towards a Standard Approach for Wear Testing of Wheel and Rail Materials*. 1–26.

Lewis, R., Olofsson, U., & Hallam, R. I. (2005). Wheel Material Wear Mechanisms and Transitions. *14th International Wheelset Congress*, 17–21.

Lewis, R., Wang, W. J., Burstow, M., & Lewis, S. R. (2016). Investigation of the influence of rail hardness on the wear of rail and wheel materials under dry conditions. *Civil-Comp Proceedings*, *110*(April). https://doi.org/10.4203/ccp.110.151

Liu, J., Jiang, W., Chen, S., & Liu, Q. (2016). Effects of rail materials and axle loads on the wear behavior of wheel/rail steels. *Advances in Mechanical Engineering*, *8*(7), 1–12. https://doi.org/10.1177/1687814016657254

Meghoe, A., Loendersloot, R., Bosman, R., & Tinga, T. (2008). *Rail Wear Estimation for Predictive Maintenance : a strategic approach*. 1–11.

Orvnäs, A. (2005). Simulation of Rail Wear on the Swedish Light Rail Line Tvärbanan. *KTH Royal Institute of Technology*.

Santamaria, J., Vadillo, E. G., & Oyarzabal, O. (2009). *Wheel-rail wear index prediction considering multiple contact patches Wheel-rail wear index prediction considering multiple contact patches*. *267*, 1100–1104. https://doi.org/10.1016/j.wear.2008.12.040

Šlapák, J., & Michálek, T. (2021). Vehicle/track interaction under the conditions of high speed railway operation. *Acta Polytechnica CTU Proceedings*, *31*(March), 45–52. https://doi.org/10.14311/APP.2021.31.0045

Telliskivi, T., & Olofsson, U. (2004). Wheel-rail wear simulation. *Wear*, *257*(11), 1145–1153. https://doi.org/10.1016/j.wear.2004.07.017

Vollebregt, E. A. H., & Wilders, P. (2011). FASTSIM2: A second-order accurate frictional rolling contact algorithm. *Computational Mechanics*, *47*(1), 105–116. https://doi.org/10.1007/s00466-010-0536-7

Zhang, D., Hu, H., Liu, Y., & Dai, L. (2014). Railway train wheel maintenance model and its application. *Transportation Research Record*, *2448*(December), 28–36. https://doi.org/10.3141/2448-04

Zhang, H., Wei, X., Guan, Q., & Zhang, W. (2022). Joint Maintenance Strategy Optimization for Railway Bogie Wheelset. *Applied Sciences*, *12*(14), 6934. https://doi.org/10.3390/app12146934

Zhang, W. (2020). Dynamic modeling of coupled systems in the high-speed train. *Dynamics of Coupled Systems in High-Speed Railways*, *1*, 55–181. https://doi.org/10.1016/b978-0-12-813375-0.00002-9